LETTERS

An optical lattice clock

Masao Takamoto[1], Feng-Lei Hong[3], Ryoichi Higashi[1] & Hidetoshi Katori[1,2]

The precision measurement of time and frequency is a prerequisite not only for fundamental science but also for technologies that support broadband communication networks and navigation with global positioning systems (GPS). The SI second is currently realized by the microwave transition of Cs atoms with a fractional uncertainty of 10^{-15} (ref. 1). Thanks to the optical frequency comb technique[2,3], which established a coherent link between optical and radio frequencies, optical clocks[4] have attracted increasing interest as regards future atomic clocks with superior precision. To date, single trapped ions[4–6] and ultracold neutral atoms in free fall[7,8] have shown record high performance that is approaching that of the best Cs fountain clocks[1]. Here we report a different approach, in which atoms trapped in an optical lattice serve as quantum references. The 'optical lattice clock'[9,10] demonstrates a linewidth one order of magnitude narrower than that observed for neutral-atom optical clocks[7,8,11], and its stability is better than that of single-ion clocks[4,5]. The transition frequency for the Sr lattice clock is 429,228,004,229,952(15) Hz, as determined by an optical frequency comb referenced to the SI second.

Accurate atomic clocks rely on the observation of a narrow atomic resonance $\Delta\nu$ at a transition frequency ν_0 that is insensitive to external perturbations to the highest possible degree. An indicator of clock performance is the fractional instability, which is minimized by repeatedly measuring the high-Q ($Q = \nu_0/\Delta\nu$) transition. The fractional instability is given by the Allan deviation[12]

$$\sigma_y(\tau) \approx \Delta\nu/(\nu_0\sqrt{N\tau}) \quad (1)$$

where N is the total number of oscillators (atoms or ions) measured in unit time and τ is the total measurement time. To improve the stability of the current Cs clock, the formula suggests the use of a transition with a higher frequency ν_0 (that is, use of higher frequency than that of microwaves), and this has led to active research towards optical clocks[4–8,11]. The use of well-designed atom traps may further increase the stability, since the extended coherent interaction time Δt reduces the Fourier limit linewidth as $\Delta\nu \approx 1/\Delta t$, thus allowing a higher effective Q-factor.

A single quantum absorber held in a space smaller than the transition wavelength[13] (that is, in the Lamb-Dicke regime) would offer the ultimate system for ultra-precise spectroscopy, as such a trap significantly decreases both atomic interactions and the Doppler shifts that critically affect clock accuracy[7,8]. This system is actually embodied by an ion in a Paul trap, where the ion is trapped at the zero of a quadrupole electric field and is not perturbed by the trapping field[14], and this has provided the finest optical spectrum yet obtained[4]. However, strong Coulomb interactions between ions prevent the use of more than a single ion in a trap, which severely limits clock stability because of small N in equation (1).

In this regard, neutral atoms with much weaker interactions[7,8,11] are suitable in terms of increasing the number of particles, and therefore the stability. A spatial interference pattern of lasers can produce periodic trapping potentials for ultracold neutral atoms, called an optical lattice[15], as illustrated in Fig. 1a. This lattice potential can confine atoms in a submicrometre region, and its periodicity allows the production of billions of micro-traps in a volume of 1 mm^3. These features are indeed attractive for fine spectroscopy with enhanced stability.

In general, such a lattice-trapping field significantly modifies the internal states of atoms by so-called light shifts, and so the system was not seriously considered for atomic clocks until the demonstration of the light shift cancellation technique[16,17]. The transition frequency ν

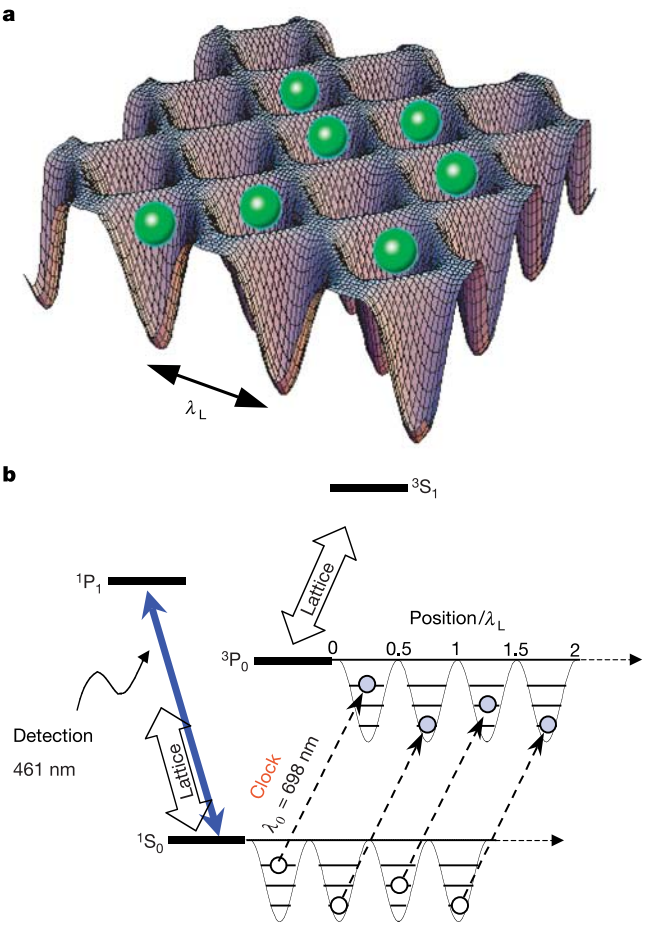

Figure 1 | Optical lattice clock. a, The spatial interference pattern of lasers creates a lattice potential that confines atoms in a region much smaller than the optical wavelength, λ_L. **b**, Energy levels for Sr. The $^1S_0$ and $^3P_0$ states are coupled to the upper respective spin states by an off-resonant laser to produce an optical lattice with equal energy shifts in the clock transition at $\lambda_0 = 698$ nm. Atoms are excited on the $|^1S_0\rangle\otimes|n\rangle \rightarrow |^3P_0\rangle\otimes|n\rangle$ electronic–vibrational transitions, where n denotes the vibrational states of atoms in the lattice potential. The clock transition is then monitored on the $^1S_0 - {}^1P_1$ cyclic transition with nearly unit quantum efficiency.

[1]Engineering Research Institute, The University of Tokyo and [2]PRESTO, Japan Science and Technology Agency, Bunkyo-ku, Tokyo 113-8656, Japan. [3]National Metrology Institute of Japan/National Institute of Advanced Industrial Science and Technology (NMIJ/AIST), Tsukuba, Ibaraki 305-8563, Japan.

of atoms exposed to a lattice laser with intensity I is given by the sum of the unperturbed transition frequency ν_0 and the light shift ν_{ac}:

$$\nu(\lambda_L, \mathbf{e}) = \nu_0 + \nu_{ac} = \nu_0 - \frac{\Delta\alpha(\lambda_L, \mathbf{e})}{2\varepsilon_0 ch} I + O(I^2) \qquad (2)$$

Here ε_0, c and h are the permittivity of free space, the speed of light and the Planck constant, respectively, and $\Delta\alpha(\lambda_L, \mathbf{e}) = \alpha_u(\lambda_L, \mathbf{e}) - \alpha_l(\lambda_L, \mathbf{e})$ is the difference between the a.c. polarizabilities of the upper and lower states (α_u and α_l, respectively), which depends both on the lattice laser wavelength λ_L and its polarization vector $\mathbf{e}$. If we adjust these polarizabilities to satisfy $\Delta\alpha(\lambda_L, \mathbf{e}) = 0$, the observed atomic transition frequency ν will be equal to ν_0 independent of the lattice laser intensity I, as long as the higher-order corrections $O(I^2)$ are negligible. In the search for a clock transition in which the light shift cancellation condition $\Delta\alpha(\lambda_L, \mathbf{e}) = 0$ can be given mainly by the laser wavelength λ_L, it is preferable to use the $J = 0$ state, which exhibits a scalar light shift and does not depend on the light polarization. These 'tricks' applied here rely on the fact that the frequency or wavelength is the most accurately measurable physical quantity, which we used to avoid measuring laser intensity or polarization.

In this experiment, we adopted the $5s^2\ ^1S_0\ (F = 9/2) \longrightarrow 5s5p\ ^3P_0\ (F = 9/2)$ forbidden transition of ^{87}Sr with a nuclear spin of 9/2 as the clock transition[9] (Fig. 1b), in which hyperfine mixing provides a finite lifetime of $\Gamma_0^{-1} = 150$ s. Our calculations[10] have shown that the $^1S_0$ and $^3P_0$ states provide an equal light shift for a lattice laser tuned to $\lambda_L \approx 800$ nm. Around this 'magic' wavelength, the light shift can be controlled with 1 mHz precision by defining the lattice laser frequency only within 1 MHz. Other systematic effects, such as the vector and tensor light shift arising from the hyperfine splitting, are summarized in the right column of Table 1 and in ref. 10. In these calculations, we assumed the typical lattice laser intensity of $I = 10\ \mathrm{kW\,cm^{-2}}$.

The experimental configuration for the lattice clock is shown in Fig. 2a (ref. 18). ^{87}Sr atoms were laser-cooled and trapped on the $^1S_0 - {}^3P_1$ transition. Roughly 10^4 atoms with a temperature of $\sim 2\ \mu$K were loaded into a 20-μK-deep one-dimensional optical lattice that was formed by the standing wave of a Ti:sapphire laser (spatially filtered by an optical fibre) and provided atoms with subwavelength confinement along the axial direction. A clock laser operating at $\lambda_0 = 698$ nm with a linewidth of ~ 10 Hz was sent into the same fibre to set its wave vector parallel to the axis of the one-dimensional lattice potential so as to satisfy the Lamb-Dicke condition. Both lasers were passed through a polarizer with an extinction ratio of 10^{-5} to guarantee linear polarization. We note that for this π-polarized lattice laser, the frequency spread due to the tensor as well as the vector light shift among Zeeman sublevels m is less than 1 mHz (ref. 10; see Table 1). The first-order Zeeman shift for $\Delta m = 0$ transitions is $m \times 106\ \mathrm{Hz\,G^{-1}}$. The residual magnetic field of 22.5 mG and random population distribution among m substates could be responsible for the Zeeman shift or broadening up to 10 Hz in this experiment. The reduction of the magnetic field down to the μG level would be feasible by applying magnetic field shielding.

We irradiated the clock laser for 10–40 ms to excite atoms trapped in the optical lattice to the $^3P_0$ state. The excitation of the clock transition was then monitored by laser-induced fluorescence on the $^1S_0 - {}^1P_1$ cyclic transition. The 'magic' wavelength for the lattice laser was determined as follows. We measured the lattice laser intensity (I)-dependent light shift ν_{ac} at several wavelengths λ_L near 813.5 nm (ref. 18), as shown in Fig. 3a. The slope of the fitted lines, which gives the differential light shift $\delta\nu_{ac}(\lambda_L, I)/\delta I$ and is proportional to the polarizability difference $\Delta\alpha(\lambda_L)$ (see equation (2)), is plotted as a function of the lattice laser wavelength λ_L in Fig. 3b. The 'magic' wavelength, where $\Delta\alpha(\lambda_L) = 0$ holds, is therefore determined as 813.420(7) nm. We note that this uncertainty introduces the scalar-light-shift uncertainty of 4 Hz (see Table 1).

The inset in Fig. 4 shows the spectrum of the clock transition at the 'magic' wavelength; each open circle was measured with an

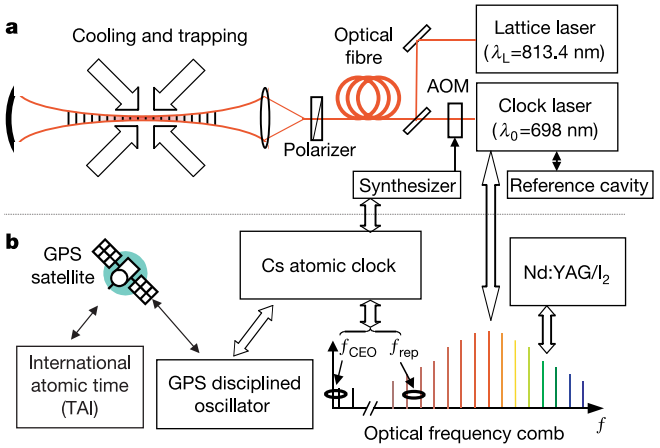

Figure 2 | Experimental configuration. a, Ultracold ^{87}Sr atoms are loaded into a one-dimensional optical lattice produced by the standing wave of a Ti:sapphire laser tuned to the 'magic' wavelength. The atoms are confined at the anti-nodes of the standing wave, which give subwavelength confinement along the axial direction. The atoms interact with the clock laser propagating along this axis, and the Lamb-Dicke condition is satisfied. AOM, acousto-optic modulator. **b**, The clock laser frequency is linked to a commercial Cs atomic clock and an iodine-stabilized Nd:YAG laser by using the optical frequency comb, where f_{CEO} and f_{rep} denote the carrier-envelope offset frequency and the repetition rate of the laser pulse, respectively. The offset frequency of the Cs clock is referenced to international atomic time through GPS time.

Table 1 | Systematic corrections and uncertainties for the Sr optical lattice clock

Effect	Correction (Hz)	Uncertainty (Hz)	
		Achieved	Attainable
First order Doppler*	0	3×10^{-2}	$<10^{-3}$
Second order Doppler	0	2×10^{-6}	$<2 \times 10^{-6}$
Recoil shift	0		
First order Zeeman	0	10	10^{-3}
Collision shift	0.6	2.4	10^{-5}†
Blackbody shift‡	2.4	0.1	3×10^{-3}
Probe laser light shift	0.1	0.01	10^{-3}
Scalar light shift	−3.8§	4	10^{-3}
Vector light shift‖	0	10^{-3}	10^{-3}
Tensor light shift	0	10^{-3}	10^{-3}
Fourth order light shift¶	0	10^{-3}	10^{-3}
Cs clock offset	−45	3	
Frequency measurement	0	9	
Systematic total	−45.7		
Total uncertainty, $\delta\nu$		15	4×10^{-3}

*The first order Doppler shift may occur owing to the relative motion between the clock laser and the lattice potential, which is often introduced by the vibration of the optical fibre or air turbulence where the clock laser travels. Taking the clock laser linewidth (~10 Hz) to be this Doppler width, the frequency uncertainty may decrease down to 30 mHz after averaging 10^5 measurements. By applying fibre phase-noise cancellation, by referring a reflection from a mirror surface that forms the standing wave for the lattice potential, this Doppler shift could be actively stabilized to less than 1 mHz (ref. 28).

†The resonant dipole–dipole interaction between atoms separately confined in the three-dimensional (3D) lattice potential with an interatomic distance of $\lambda_L/2 \approx 400$ nm is assumed[10].

‡The blackbody shift scales as $\nu_B \approx 3 \times 10^{-10} \times T^4$ Hz (where T is in units of K), which would introduce 3 mHz uncertainty for the temperature inhomogeneity of $\Delta T = 0.1$ K at $T = 293$ K.

§The measurements in Fig. 4 were carried out with the lattice laser wavelength at 813.4270 nm, which was finally found to be 0.007 nm longer than the actual 'magic' wavelength. The Stark shift introduced by this wavelength difference is corrected.

‖In realizing 3D optical lattices, one can apply a phase stable optical lattice where the 3D laser intersection is formed by a single linearly polarized standing-wave with folded mirrors[29]. In this configuration, since the amplitude and the phase of the trapping light fields are correlated in each lattice site, the high polarization stability is expected.

¶This is estimated without including the resonant contribution[10].

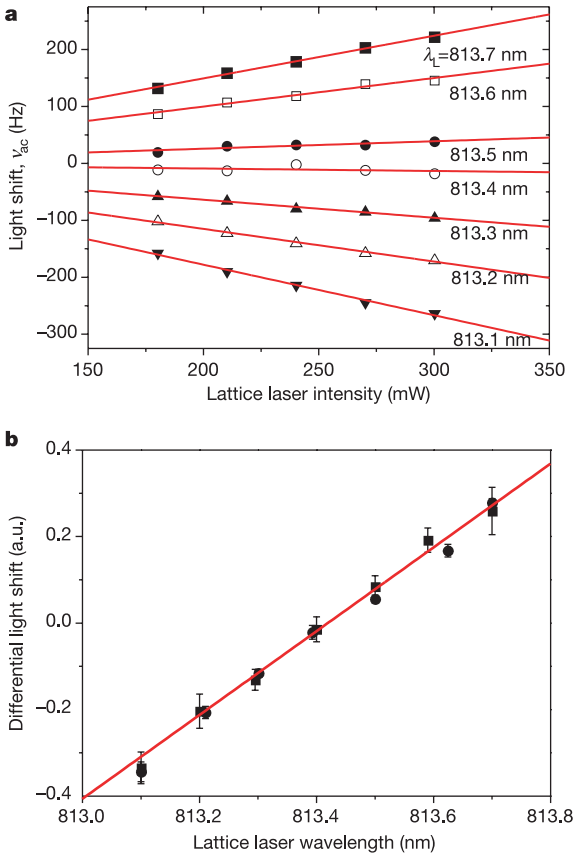

Figure 3 | Determination of the 'magic' wavelength. **a**, The light shift ν_{ac} of the clock transition was measured as a function of the lattice laser intensity I at several wavelengths λ_L near 813.5 nm. The differential light shift $\delta\nu_{ac}/\delta I$ was determined by the slope of the fitted lines. **b**, The differential light shift, which is proportional to the dipole polarizability difference $\Delta\alpha(\lambda_L)$, is plotted as a function of the lattice laser wavelength λ_L. The error bars represent the standard error. The 'magic' wavelength, where $\Delta\alpha(\lambda_L) = 0$, was determined to be $\lambda_L = 813.420(7)$ nm by a linear fit to the data points. a.u., arbitrary units.

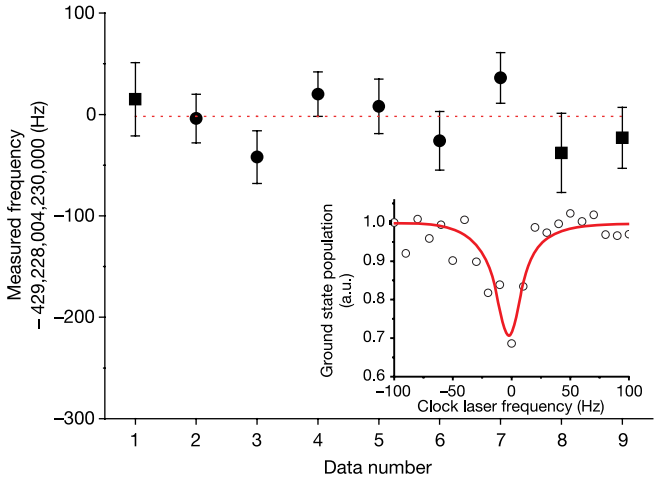

Figure 4 | Absolute frequency measurement of the $^1S_0 - {}^3P_0$ transition of Sr atoms in an optical lattice. The inset shows the typical clock transition resolving a linewidth of 27 Hz. The resonance frequency was measured by an optical frequency comb generator referenced to a commercial Cs clock. Each filled square/circle corresponds to a frequency measurement over 10^4 s. The standard deviation of the mean, which is typically 28 Hz, is shown by error bars. The filled circles correspond to measurements with an iodine-stabilized Nd:YAG laser as a flywheel, discussed in Methods. The 9 days of measurement determined the clock transition to be 429,228,004,229,952(15) Hz, applying the systematic correction of −45.7 Hz to the data shown in the figure.

interrogation time of 40 ms and a cycle time of 1 s, which is required for cooling, trapping and spectroscopy. We observed a nearly Fourier-limited linewidth of 27 Hz, which is the narrowest linewidth yet reported for neutral-atom-based optical clocks[7,8,11]. With 20 data points that took ~20 s to measure, the lorentzian fitting of the spectrum determined the centre frequency with an uncertainty of 2 Hz, corresponding to an Allan deviation $\sigma_y \approx 10^{-14}$ at $\tau = 1$ s. With the present measurement, the signal to noise ratio is limited by the shot-to-shot fluctuation (~10%) in the number of atoms loaded into the optical lattice. Normalization of the excitation rate[7], in addition to reduction of the clock laser linewidth[19], would improve the clock stability towards the projection noise limit for 10^6 atoms[1,7] of $\sigma_y(\tau) \approx 10^{-18}/\sqrt{\tau}$ (ref. 10), with τ measured in seconds.

The schematic for the absolute frequency measurement is shown in Fig. 2b. We repeated the above scan to determine the atomic resonance every 20 s and recorded the slow drift (~0.1 Hz s^{-1}) of the reference cavity that was used to prestabilize the clock laser. Simultaneously, we used the frequency comb, and measured the clock laser frequency against a commercial Cs clock (Agilent 5071A) that was calibrated with international atomic time (TAI) through GPS time[20]. These two sets of data were combined to deduce the absolute frequency of the lattice clock, as summarized in Fig. 4. In the figure, each filled square/circle represents a frequency measurement of typically 10^4 s to reduce the fractional instability of the Cs clock down to 6.5×10^{-14}, corresponding to an uncertainty of 28 Hz. With a total averaging time of $\tau \approx 9.4 \times 10^4$ s over 9 days, we reached an uncertainty of 9 Hz. The sources of the uncertainties and the corrections are listed in Table 1, and give a final value of 429,228,004,229,952(15) Hz, which is consistent with a measurement reported by Courtillot *et al.*[21] within their measurement uncertainty of 20 kHz. The collisional frequency shift, which was measured by varying the atom density by a factor of 3, was less than a measurement uncertainty (see Table 1). However, the shift may be present in this one-dimensional lattice configuration, as tens of atoms were typically trapped in a single lattice potential with an atom density of ~10^{12} cm^{-3}. This collision shift could ultimately be removed by spin-polarizing the ^{87}Sr atoms to activate the Fermi suppression of collisions[22], or by applying a three-dimensional lattice[9,10] with less than unity occupation, as shown in Fig. 1a.

This lattice clock scheme is applicable to other divalent atoms that have a hyperfine-mixing induced $J = 0 \rightarrow J = 0$ transition between long-lived states, such as ^{43}Ca (ref. 23), ^{171}Yb (ref. 24) and ^{199}Hg, in addition to the ^{87}Sr used here. A frequency comparison of lattice clocks operated with different atomic species would allow us to study the time variation of the fine structure constant[25]. The very high potential stability of this scheme would enable us to measure the fractional frequency difference at the 10^{-18} level, which corresponds to the gravitational red shift for a 1 cm height difference, in only one second. We expect that these features will have a great effect on future metrology, in areas ranging from fundamental physics to aspects of engineering, such as the remote sensing of natural resources.

METHODS

Optical frequency measurement. The development of ultrafast laser technology has revolutionized research on optical frequency measurement by introducing a precise optical frequency comb based on a femtosecond mode-locked laser[2]. The frequency of the nth comb component is expressed as $f_n = (n \times f_{rep}) + f_{CEO}$, where f_{rep} is the repetition rate of the laser pulse and f_{CEO} is the carrier-envelope offset frequency (Fig. 2b). The frequency comb obtained by injecting light from a mode-locked laser into a photonic crystal fibre[26] can cover more than one octave across the visible and near-infrared regions. f_{CEO} was measured directly with an

f-to-2f interferometer in the octave-spanning comb[3]. When f_{rep} and f_{CEO} are precisely controlled, the comb works as a 'frequency linker' that connects optical and radio frequencies. In the present experiment, a mode-locked Ti:sapphire laser with a repetition rate of 793 MHz was used to generate a frequency comb covering the 500–1,100 nm range. The frequency measurement was implemented by phase-locking the whole comb to the Sr clock laser and measuring f_{rep} against the Cs clock.

The frequency f_c of the clock laser prestabilized to a stable high-finesse reference cavity was frequency-scanned with an acousto-optic modulator (AOM) to find the atomic resonance frequency ν_0 every 20 s by observing a spectrum as shown in the inset of Fig. 4. As the frequency setting of the AOM $\delta(t) = f_c(t) - \nu_0$ measured the temporal drift of the clock laser, the atomic resonance frequency ν_0 could be determined by simultaneously measuring the clock-laser frequency $f_c(t)$. We observed a beat frequency $f_b = |f_c - f_n|$ between the clock laser and the nth comb component at 698 nm, and used it to servo-control the f_{rep} of the comb. Consequently, the clock-laser frequency $f_c(t)$ was converted to f_{rep}, which was then mixed down to about 7 MHz and recorded by a frequency counter with a gate time of 20 s. The clock-laser frequency $f_c(t)$ was calculated by using the formula $f_c = (n \times f_{rep}) + f_{CEO} \pm f_b$ with an integer $n \approx 5.4 \times 10^5$. The ambiguous sign was removed by observing the sign of the variation in the beat frequency f_b while f_{rep} was varied. We have thus obtained two series of data sets; the offset frequency $\{\delta(t)\}$ and the corresponding clock-laser frequency $\{f_c(t)\}$, both of which were determined every $t_m = 20$ s. The atomic resonance frequency was calculated as $\nu_0(k) = f_c(kt_m) - \delta(kt_m)$ for $k = 1, 2, \ldots, k_{max}$, where $k_{max} = T_{max}/t_m$ with T_{max} typically 10^4 s. Each filled square in Fig. 4 represents the mean value of $\{\nu_0(k)\}$, whose standard deviation of $\sigma \approx 620$ Hz was in agreement with the Cs clock's instability at $\tau = 20$ s. The standard deviation of the mean $\sigma/\sqrt{k_{max}}$ gave error bars of about 28 Hz.

In an alternative experimental scheme, a transportable iodine-stabilized Nd:YAG laser (NMIJ-Y1)[27] was used as a flywheel in the frequency measurement. The instability of the Nd:YAG laser $\sigma_y(\tau)$ is 2×10^{-13} for $\tau = 1$ s. This value improves after $\tau = 100$ s towards 3×10^{-14}, which is smaller than that of the Cs clock until $\tau = 10^5$ s. Furthermore, $\sigma_y(\tau)$ of the Nd:YAG laser is smaller than that of the clock laser for $\tau > 30$ s, which makes it possible to observe the slow drift of the clock laser. Because of the excellent short-term stability of the Nd:YAG laser, we also performed a frequency measurement by phase-locking the comb to the Nd:YAG laser. The clock-laser frequency $f_c(t)$ was measured by simultaneously introducing a second beat measurement between the clock laser and the comb component at 698 nm. The measurement results obtained with this scheme coincide with those obtained with the first measurement scheme, and are indicated by filled circles in Fig. 4.

The frequency of the Cs clock was monitored by the GPS time during the period of the frequency measurement (over one month). The timing difference between the 1 p.p.s. (pulse per second) signals generated by the Cs clock and a GPS disciplined oscillator was recorded continuously by a time interval counter. The frequency offset between the Cs clock and the GPS time was calculated from the recorded timing difference and found to be $-1.04(8) \times 10^{-13}$. The relationship between GPS time and TAI is available[20]. The agreement between the GPS time and the TAI was about one part in 10^{15} during the period of the frequency measurement.

Received 7 December 2004; accepted 10 March 2005.

1. Pereira Dos Santos, F. *et al.* Controlling the cold collision shift in high precision atomic interferometry. *Phys. Rev. Lett.* **89,** 233004 (2002).
2. Udem, Th., Reichert, J., Holzwarth, R. & Hänsch, T. W. Absolute optical frequency measurement of the cesium D_1 line with a mode-locked laser. *Phys. Rev. Lett.* **82,** 3568–3571 (1999).
3. Jones, D. J. *et al.* Carrier-envelope phase control of femtosecond mode-locked lasers and direct optical frequency synthesis. *Science* **288,** 635–639 (2000).
4. Diddams, S. A. *et al.* An optical clock based on a single trapped $^{199}Hg^+$ ion. *Science* **293,** 825–828 (2001).
5. Peik, E. *et al.* Limit on the present temporal variation of the fine structure constant. *Phys. Rev. Lett.* **93,** 170801 (2004).
6. Margolis, H. S. *et al.* Hertz-level measurement of the optical clock frequency in a single $^{88}Sr^+$ ion. *Science* **306,** 1355–1358 (2004).
7. Wilpers, G. *et al.* Optical clock with ultracold neutral atoms. *Phys. Rev. Lett.* **89,** 230801 (2002).
8. Oates, C. W., Curtis, E. A. & Hollberg, L. Improved short-term stability of optical frequency standards: approaching 1 Hz in 1 s with the Ca standard at 657 nm. *Opt. Lett.* **25,** 1603–1605 (2000).
9. Katori, H. in *Proc. 6th Symp. on Frequency Standards and Metrology* (ed. Gill, P.) 323–330 (World Scientific, Singapore, 2002).
10. Katori, H., Takamoto, M., Pal'chikov, V. G. & Ovsiannikov, V. D. Ultrastable optical clock with neutral atoms in an engineered light shift trap. *Phys. Rev. Lett.* **91,** 173005 (2003).
11. Ruschewitz, F. *et al.* Sub-kilohertz optical spectroscopy with a time domain atom interferometer. *Phys. Rev. Lett.* **80,** 3173–3176 (1998).
12. Allan, D. W. Statistics of atomic frequency standards. *Proc. IEEE* **54,** 221–230 (1966).
13. Dicke, R. H. The effect of collisions upon the Doppler width of spectral lines. *Phys. Rev.* **89,** 472–473 (1953).
14. Dehmelt, H. G. Mono-ion oscillator as potential ultimate laser frequency standard. *IEEE Trans. Instrum. Meas.* **31,** 83–87 (1982).
15. Jessen, P. S. & Deutsch, I. H. in *Advances in Atomic, Molecular and Optical Physics* Vol. 37 (eds Bederson, P. & Walther, H.) 95–138 (Academic, San Diego, 1996).
16. Katori, H., Ido, T. & Kuwata-Gonokami, M. Optimal design of dipole potentials for efficient loading of Sr atoms. *J. Phys. Soc. Jpn* **68,** 2479–2482 (1999).
17. Ido, T. & Katori, H. Recoil-free spectroscopy of neutral Sr atoms in the Lamb-Dicke regime. *Phys. Rev. Lett.* **91,** 053001 (2003).
18. Takamoto, M. & Katori, H. Spectroscopy of the $^1S_0 - {}^3P_0$ clock transition of ^{87}Sr in an optical lattice. *Phys. Rev. Lett.* **91,** 223001 (2003).
19. Young, B. C., Cruz, F. C., Itano, W. M. & Bergquist, J. C. Visible lasers with subhertz linewidths. *Phys. Rev. Lett.* **82,** 3799–3802 (1999).
20. Bureau International des Poids et Mesures (BIPM), Circular T, No. 200 ⟨http://www1.bipm.org/en/scientific/tai/time_ftp.html⟩ (August 2004).
21. Courtillot, I. *et al.* Clock transition for a future optical frequency standard with trapped atoms. *Phys. Rev. A* **68,** 030501 (2003).
22. Gupta, S. *et al.* Radio-frequency spectroscopy of ultracold fermions. *Science* **300,** 1723–1726 (2003).
23. Degenhardt, C., Stoehr, H., Sterr, U., Riehle, F. & Lisdat, C. Wavelength-dependent ac Stark shift of the $^1S_0 - {}^3P_1$ transition at 657 nm in Ca. *Phys. Rev. A* **70,** 023414 (2004).
24. Porsev, S. G., Derevianko, A. & Fortson, E. N. Possibility of an optical clock using the $6^1S_0 \rightarrow 6^3P_0^0$ transition in $^{171,173}Yb$ atoms held in an optical lattice. *Phys. Rev. A* **69,** 021403 (2004).
25. Angstmann, E. J., Dzuba, V. A. & Flambaum, V. V. Relativistic effects in two valence-electron atoms and ions and the search for variation of the fine-structure constant. *Phys. Rev. A* **70,** 014102 (2004).
26. Knight, J. C. Photonic crystal fibres. *Nature* **424,** 847–851 (2003).
27. Hong, F.-L. *et al.* Frequency comparison of $^{127}I_2$-stabilized Nd:YAG lasers. *IEEE Trans. Instrum. Meas.* **48,** 532–536 (1999).
28. Ma, L.-S., Jungner, P., Ye, J. & Hall, J. L. Delivering the same optical frequency at two places: accurate cancellation of phase noise introduced by an optical fiber or other time-varying path. *Opt. Lett.* **19,** 1777–1779 (1994).
29. Rauschenbeutel, A., Schadwinkel, H., Gomer, V. & Meschede, D. Standing light fields for cold atoms with intrinsically stable and variable time phases. *Opt. Commun.* **148,** 45–48 (1998).

Acknowledgements We thank M. Yasuda, Y. Fukuyama and J. Jiang for assistance with the experiments, and A. Onae and S. Ohshima for discussions. This work was supported by the Strategic Information and Communications R&D Promotion Programme (SCOPE) of the Ministry of Internal Affairs and Communications of Japan.

Author Information Reprints and permissions information is available at npg.nature.com/reprintsandpermissions. The authors declare no competing financial interests. Correspondence and requests for materials should be addressed to H.K. (katori@amo.t.u-tokyo.ac.jp).